5G NOMA Defense Application Environment and Stacked LSTM Network Architectures

Ravi Shankar[1,*], Manoj Kumar Beuria[2], Sudhansu Sekhar Singh[2], Farkhanda Ana[3], Haider Mehraj[3] and V. Gokula Krishnan[4]

[1]*Madanapalle Institute of Technology and Science, Madanapalle, Andhra Pradesh, India*
[2]*Kalinga Institute of Industrial Technology University, Odisha, India*
[3]*Department of Electronics and Communication Engineering, Baba Ghulam Shah Badshah University, Rajouri, J&K, India – 185234*
[4]*Department of Computer Science and Engineering, Saveetha School of Engineering, Saveetha Institute of Medical and Technical Sciences, Thandalam, Chennai – 602105, Tamil Nadu, India*
E-mail: ravi.mrce@gmail.com; gokul_kris143@yahoo.com
[*]*Corresponding Author*

Received 23 November 2021; Accepted 11 May 2022;
Publication 25 August 2022

Abstract

In 5G and beyond 5G wireless communication networks, the NOMA scheme is widely considered a major non-orthogonal access technique for improving system capacity and data rates. The main challenges in current NOMA systems are limited channel feedback and the difficulty of integrating it with advanced adaptive coding and modulation algorithms. This study analyses S-LSTM-based DL NOMA receivers in i.i.d. Nakagami-m fading channel circumstances as opposed to previously presented solutions. The LSTM has the advantage of responding dynamically to changing channel conditions. When compared to a typical NOMA system, a typical NOMA system has a 12% lower outage probability, a 39% increase in net throughput, and a maximum SER reduction of 48%. Complex modulated M-*ary* PSK and M-*ary* QAM data symbols are employed in D/L NOMA transmission. Classic

Journal of Mobile Multimedia, Vol. 19_1, 73–102.
doi: 10.13052/jmm1550-4646.1914

receivers such as LS and MMSE are outperformed by the S-LSTM-based DL-NOMA receiver. The CP and non-linear clipping noise simulation curves compare the performance of the MMSE and LS receivers with that of the DL NOMA receiver in real-time propagation circumstances. The DL-based detector outperforms the MMSE for SNRs greater than 15 dB because the S-LSTM method is more robust than the clipping noise.

Keywords: 5G, NOMA, B5G, PAPR, DNN, Nakagami-m fading channel, RNN, S-LSTM Fourier transform.

Acronym	Explanation
5G	Fifth-generation of wireless communication
ISI	Inter-symbol interference
DNN	Deep neural network
SE	Spectral efficiency
SER	Symbol error rate
STBC	Space-time block code
BS	Base station
UE	User equipment
IoT	Internet of things
SIC	Successive interference cancellations
D/L	Downlink
DL	Deep learning
MIMO	Multiple input multiple output
LSTM	Long short-term memory
AWGN	Additive white Gaussian noise
NOMA	Non-orthogonal multiple access
mmWave	millimeter wave
CSI	Channel state information
MEC	Mobile edge computing
ML	Machine learning
S-LSTM	Stacked Long short-term memory
IID	Independent and identically distributed
B5G	Beyond fifth-generation wireless network
SWIPT	Simultaneous wireless information and power transfer
ReLU	Rectified linear unit
FT	Fourier transform

Acronym	Explanation
CP	Cyclic prefix
OFDM	Orthogonal frequency division multiplexing
RNN	Recurrent neural network
PSK	Phase shift keying
FV	Feature vector
QAM	Quadrature
AI	Artificial intelligence
MATLAB	Matrix laboratory
MMSE	Minimum mean square error
OMA	Orthogonal multiple access
LS	Least-squares
SNR	Signal to noise ratio
PS	Pilot symbols
LR	learning rate
CD	Clipping distortion
PAPR	Peak to average power ratio
VLC	Visible light communication
MA	Multiple access
U/L	Uplink

1 Introduction

Military communications specialists are working hard to bring 5G [1–4] technology to the battlefield's front lines to offer high-speed sensor, targeting, and intelligence data to front-line combat fighters. 5G data rates of gigabits per second, ultra-low latency, massive capacity, more efficient coordination, and increased dependability [5, 6]. The 5G technology specifications and the 5G-IoT networks are presented in Figs. 1 and 2, respectively. Despite extensive research to address the SE problem, SE has become a highly demanding issue as the number of devices connected to 5G and IoT networks grows [7, 8]. More effective MA methods have lately been researched in 5G and B5G approaches to provide significantly greater data transmission rates and huge connections. Figure 3 depicts a schematic representation of 5G with military communication. NOMA is a well-known MA approach for enhancing system performance while also increasing network connection density [9]. Interference among cellular users is a significant issue that must be addressed in 5G networks. Unlike previous MA systems, which assigned the radio spectrum to each cellular user based on orthogonal codes and space-time trellis codes to

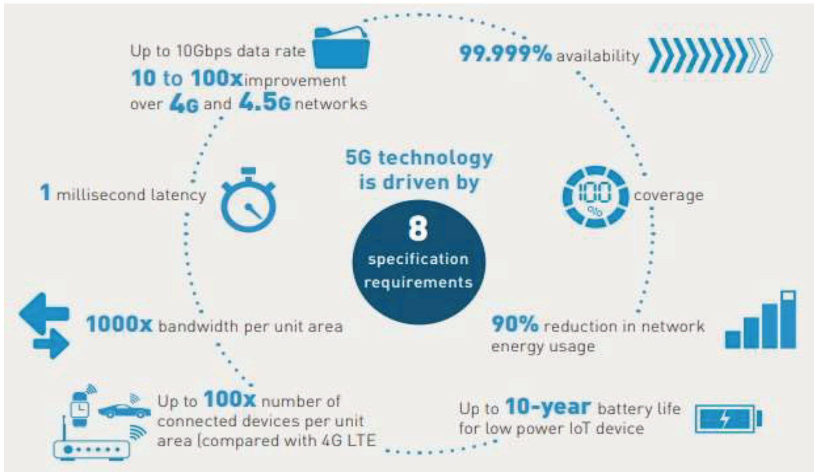

Figure 1 5G Technology specifications.

prevent ISI, NOMA distributes identical transmission resources to all users in a non-orthogonal manner [10]. This allows for non-orthogonal user stacking, which allows multiple users to share transmission resources at the same time. The NOMA concept is used to distribute power to the BS. In other words, UEs with high channel gains are given less power, while those with low channel gains are given more power for better SER performance. The composite signal that results from the signals of all UEs is then superimposed at the BS, resulting in the composite signal that is broadcast over the channel [11]. Cellular users having low channel strengths (high power is allocated) detect their information by considering all other UE signals as noise, but users with high channel gain (low power is allocated) must perform SIC, as illustrated in Figure 4 [11].

SIC's purpose is to estimate a specific user's signal based on a received superposed signal from the BS. This is accomplished by first decoding the signal(s) of users with higher power levels, then removing them from the superposed signal and decoding the difference as the UE with a lower power level.

Because of the transmission and reception activities, a NOMA-based system model can assist 5G communication systems with massive connectivity and high data rates. Power and spectrum are typically allocated separately. The performance of the conventional NOMA system suffers in the situation of joint resource allocation due to limited spectrum availability. To solve

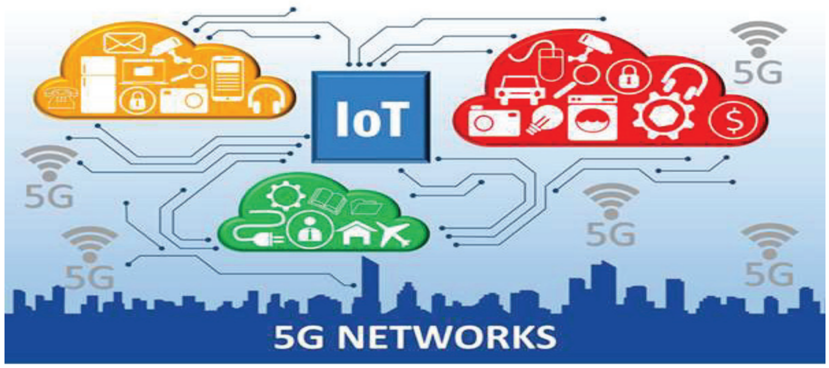

Figure 2 The schematic representation of the 5G-IoT network.

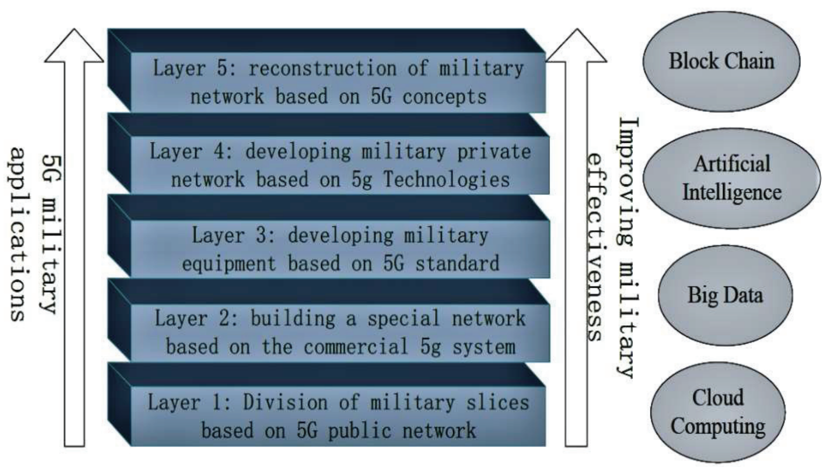

Figure 3 5G Military application scenario.

this optimization challenge, the authors have proposed several suboptimal solutions [12, 13]. At the same time, the solution space for the optimization issue is large, necessitating the employment of nonlinear search techniques. As a result, standard strategies for solving this optimization problem are insufficient and unreliable in getting sufficient channel assignment, limiting the performance of the NOMA system. The AI/ML scheme offers new ways to create 5G wireless networks, which have become a hotspot for research in the communications industry [14, 15]. As illustrated in Figure 5 [16], DL has lately gained popularity as a beneficial technique for incorporating into wireless communication systems, hence improving system design.

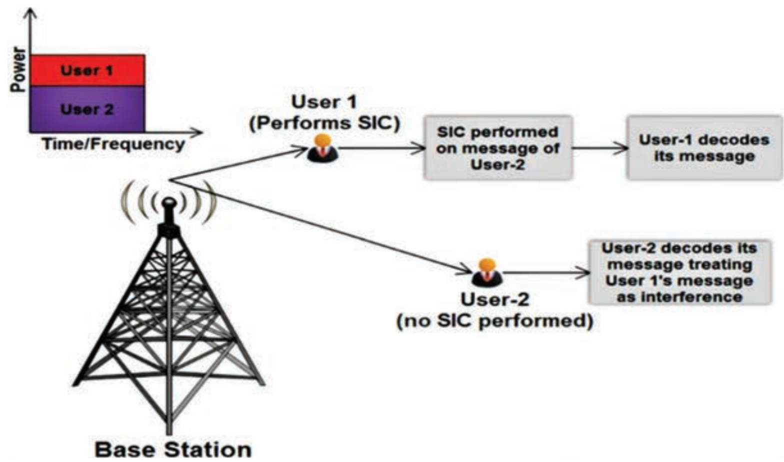

Figure 4 Schematic representation of the D/L power domain NOMA scheme.

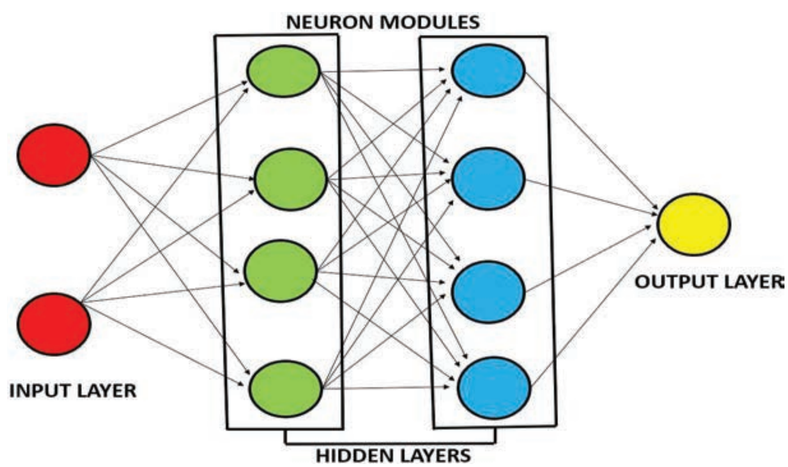

Figure 5 Schematic representation of the DNN network.

The nonlinear relationship in the training data is maximized by DL, which increases system performance. The authors have provided a detailed account of the function of DL in power allocation in NOMA systems in their study [16], which was prompted by DL's potential. The LSTM network is used to create DL aided NOMA system that can intelligently detect fading channel coefficients [17]. In the work [18], a DNN is used to build the MIMO-NOMA system's precoder and SIC decoder. Precoding and SIC decoding in the MIMO-NOMA system are optimized concurrently, allowing the incoming signal to be successfully decoded. Due to its excellent feature learning capacity, the application of DL to signal detection, particularly modulation classification, has piqued the interest of most researchers [19, 20]. In work [18], when the network's input data includes baseband signals, the performance gain of typical DNN topologies for modulation classification is comparable. For neural networks to improve their recognition ability, more discriminative representations of modulated signals must be found. The constellation diagrams and spectrogram images are input into convolutional neural networks in [19, 20].

The current 5G-NOMA networks have a significant disadvantage: high computational complexity combined with an i.i.d. Nakagami-m fading channel makes leveraging the channel's features and determining the best allocation methodologies extremely challenging. To address this fundamental constraint, we suggested in this paper a novel and successful DL-assisted NOMA system in which a single BS supports many NOMA users via random deployment. The DL method is used to improve end-to-end system performance since it allows us to train input signals and recognize rapidly fluctuating channel coefficients. The NOMA system will use it to learn a completely new channel environment. The suggested technique uses an S-LSTM NOMA system to detect fading channel coefficients automatically. The suggested technique involves offline learning to train the S-LSTM using simulated data under various channel circumstances, then online learning to acquire the matching output data using the current input data. To perform automatic encoding, decoding, and channel detection in an AWGN channel, we develop, train, and test the recommended cooperative framework. Furthermore, we take an unknown nonlinear mapping operation to be one frequent user activity and data detection approach, and we use S-LSTM to approximate it to evaluate DL's NOMA data detection capabilities. Simulation findings demonstrate that the proposed approach is both durable and efficient when compared to established techniques. Using the well-known tenfold cross-validation method, the accuracy of the S-LSTM-assisted NOMA scheme is also evaluated. To increase the efficacy and dependability of the NOMA system based on the DL technique, extensive research has been conducted.

The following are the major contributions of this study.

- *To the best of our understanding, by using DL to build a NOMA system, we are attempting to assess the complicated channel properties of NOMA using DL approaches rather than regular online learning. The* *pre-training approach for the DL network has been altered to increase the DL framework's performance.*

- *In this paper, we provide a system that uses the S-LSTM (a common branch of DNN) and NOMA to incorporate the LSTM into NOMA. The suggested approach can automatically get the CSI of the i.i.d. Nakagami-m fading channel. Meanwhile, we utilize the S-LSTM network, which is based on the U/L NOMA system, to solve this non-convex optimization issue and increase the end-to-end reliability, provide lower latency and reduce the computing time of unique user activity and data recognition approaches. As a result, it has been proven that DL may be used in NOMA network data detection optimization and U/L analysis.*
- *We examine the performance of the recommended DL-based techniques in the NOMA system for generalized fading channel scenarios. The net throughput, as well as the SER, are extensively examined. Furthermore, extensive simulation results and comparisons demonstrate that the proposed solutions are effective and robust.*

2 Related Works

In the work [21], the authors presented a detailed examination of DL-assisted wireless communication. The evolution and significance of DL are examined. The authors discuss the importance of DL in potential wireless methods such as NOMA, cooperative communication, massive Machine-Type Communications, mmWave, and ultra-reliable low-latency communications. They also discuss the problems, possibilities, and future research directions for DL in the current 5G and B5G wireless environment. They show how the DL-assisted NOMA system may improve SE, channel capacity, and CSI. In the work [22], the authors have analyzed the NOMA's role in the 5G and B5G wireless systems. The authors have investigated the advantages of NOMA in detail, as well as how NOMA works with other technologies, including massive MIMO, relaying communication, mmWave communication, cognitive relaying network, SWIPT, wireless data privacy and security, VLC, and MEC. It also outlines the research directions for NOMA's collaboration with other wireless technologies, as well as technical contributions. In the work [23], the authors have considered the D/L NOMA system by considering a two-user single cell to a *k*-user multi-cell network with OMA schemes. The authors conducted a thorough investigation of the NOMA system and presented many optimization strategies for improving the system's SE. SIC, power allocation factor, CSI, and interchannel interference are all examined in length as different elements and issues in the NOMA system. The impact of AI, ML, and DL on 5G and B5G generation NOMA systems is also discussed.

In the work [24], the authors have demonstrated the advantages of the NOMA system when combined with DL algorithms. The authors evaluate the practicality of DL and present a detailed study of wireless communication issues. Optimal resource and power allocation, channel and signal identification, and sophisticated modulated signal constellation design are the three aspects of the study. The work [24] discusses the limits and limitations of DL-assisted NOMA in wireless communication systems. In the work [25], the author examines the most recent research in wireless and IoT networks in depth. In large, networked devices, the authors investigate the interference management, channel assignment, user pairing, clustering, and network coverage expansion issues. The concepts of DL schemes are also covered, as well as the variety of DL algorithms used in resource management for 5G-IoT assisted networks. DNNs of various varieties, as well as their recent contributions to wireless communication challenges, are discussed in detail. The paper adds to the study and knowledge of 5G and B5G schemes such as Coordinated Multi-Point transmission and reception, NOMA, heterogeneous networks, and machine-to-machine communication.

In the previous works [26–28], the authors have employed the DL to investigate the physical layer security, channel modeling, and coding of the MIMO system. In the work [29], the authors have investigated a DL-aided sparse code MA strategy in which the codebook that minimizes the SER is adaptively constructed, which requires less time to calculate than conventional schemes. The authors of the paper [30] developed a MIMO OFDM system using the DL in an OFDM scenario, and its increased performance in terms of channel estimation and signal identification has been demonstrated. In the works [31–34], the DL algorithm has been used in traffic control systems, and some of the benefits of DL-based communication systems have been examined.

The authors investigated a multiple user D/L MIMO-NOMA network in their paper [37]. The PS is employed in the simulations to identify the channel coefficients, and a DNN based CSI and channel detection is constructed based on these pilot responses, and net throughput is studied. The suggested DNN system outperforms the classic SIC-based NOMA channel detector, according to the simulation findings. In the work [38], the authors devised a DL-based mathematical framework to conduct channel identification in a MIMO-based NOMA network under frequency flat fading channel scenarios considering imperfect CSI. The proposed method can calculate fading channel coefficients and recognise signals at the same time. In terms of BER and channel capacity, the proposed DNN scheme is simulated, and the results are compared to the traditional SIC system. According to the simulation results, the suggested DL-based technique can overcome fading channel imperfection even though the studied NOMA cell was limited to only two users and needed an offline training stage.

2.1 Proposed DL Algorithm

We use the S-LSTM technique to investigate the generalized i.i.d. Nakagami-m fading channel conditions because it allows us to train input signals and automatically detect the fading channel coefficients in the case of real-time propagation scenarios. It is used in the proposed NOMA system to learn a line of sight fading channel environment. An S-LSTM network based on DL is incorporated into a traditional NOMA system, allowing the proposed method to automatically detect fading channel coefficients. The suggested technique involves training the S-LSTM using simulated data under various channel circumstances via offline learning and then obtaining the matching output data using the current input data utilized during the online learning process. We build, train, and evaluate the proposed cooperative framework to conduct automated detection of channel coefficients, channel encoding, and decoding under the AWGN channel. Furthermore, we analyze an unknown nonlinear mapping operation, which we approximate with S-LSTM to evaluate the data detection capabilities of DL based on NOMA, as one typical user activity and data detection technique. Simulation findings reveal that the proposed approach is both reliable and efficient when compared to established techniques. Using the well-known 10-fold cross-validation technique, the accuracy of the S-LSTM-assisted NOMA scheme is evaluated as well. This research uses the S-LSTM algorithm, which is a kind of RNN. The NOMA OFDM system is integrated with the S-LSTM to obtain the best SER performance throughout the i.i.d. Nakagami-*m* fading channel situations. Using an S-LSTM-based NOMA OFDM detector instead of a traditional SIC NOMA detector results in a 10% reduction in OP, a 37% increase in net throughput, and a maximum 50% reduction in SER.

2.2 Paper Organization

The system model and the OFDM transmitter and receiver block diagram are appropriately discussed in Section 2 of this study. The DL NOMA receiver is investigated in Section 3, and the S-LSTM design is presented in this section. Section 4 presents the simulation results, while Section 5 concludes the article. Finally, Section 6 discusses the obstacles and future research prospects for the suggested technology.

3 System Model

3.1 S-LSTM Basics

In this subsection, we consider the NOMA OFDM detector based on the S-LSTM algorithm. S-LSTM is a subset of the DNN. Because of the time delays introduced by unknown periods, S-LSTM is an excellent tool for analyzing, classifying, and forecasting time series. After fixing the number of training sets, the S-LSTM will increase the SER performance by utilizing the hidden layers. The S-LSTM is an efficient technique for complex data processing.

3.1.1 S-LSTM algorithm is given below [32–37]

Inputs: Transmitted pilot data, s_m, for cellular users, target fading channel matrices, z_m.

1: *Randomly initialize the weights (B's) and bias (w's) values*.
2: *The forget gate*: $\Upsilon_n = sigmoid(\sum_{n=1}^{3000} B_\Upsilon Z_{n-1} + B_\Upsilon s_n + w_\Upsilon)$
3: *The input gate*: $m_n = sigmoid(\sum_{n=1}^{3000} B_m Z_{n-1} + B_m s_n + w_m)$
4: *The candidate value*: $\tilde{C}_n = tanh(\sum_{n=1}^{3000} B_c H_{n-1} + B_c s_n + w_c)$
5: *Update the old cell state, C_{n-1}, into the new cell state, C_n, by*: $C_n = (C_{n-1} \times \Upsilon_n) + (m_n \times \tilde{C}_n)$
6: *Update the output of the S-LSTM by*: $o_n = sigmoid(\sum_{n=1}^{3000} B_o Z_{n-1} + B_o s_n + w_o)$
The estimated channel matrix: $z_n = o_n \times \tanh(C_n)$
Outputs: Estimated channel matrices, Z_n, and the equivalent SNR values.

The conventional S-LSTM algorithm is made up of several hidden layers, an input layer, and an output layer. The hidden S-LSTM layer, unlike a conventional RNN, has many gate units to regulate data flow [30–36]. Figure 6 shows a schematic representation of the S-LSTM algorithm with proper labeling.

The limited Boltzmann machine network manages the input layer, whereas the sigmoid function manages the output layer. The ReLU [8, 9] function is used to further process all hidden layers.

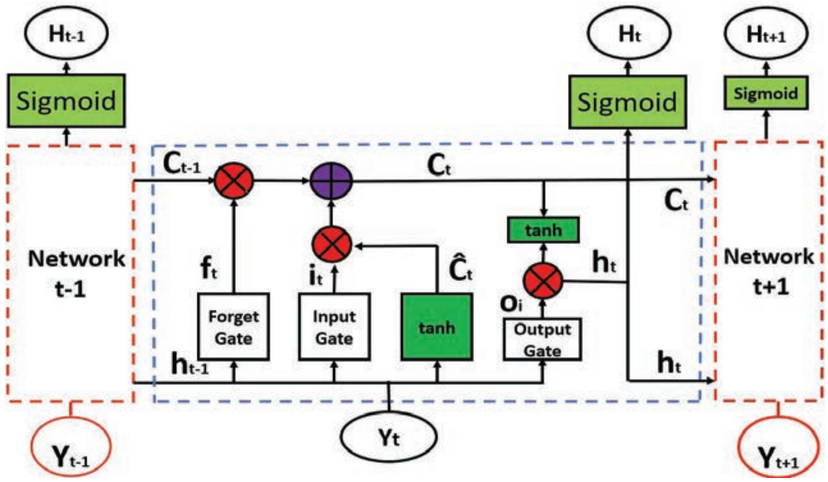

Figure 6 The schematic block diagram demonstration of the S-LSTM architecture.

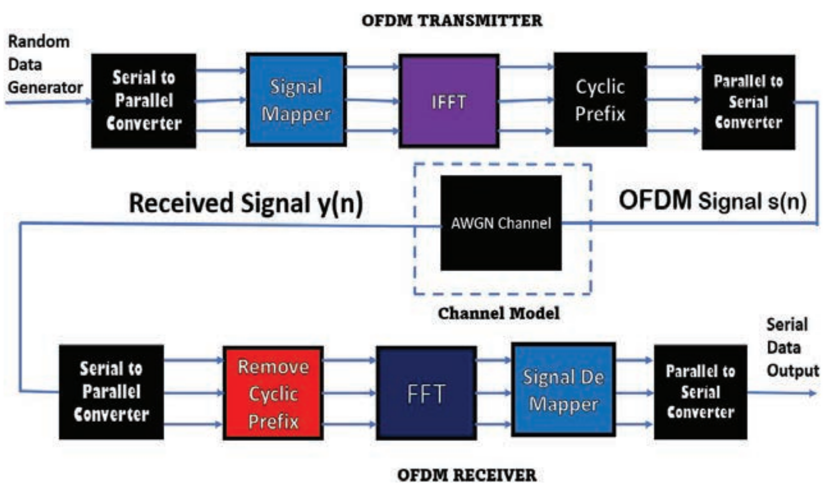

Figure 7 OFDM signal transmission considering AWGN channel [12].

3.1.2 OFDM signal transmission

The OFDM signal transmission is suitably represented in Figure 7. Digital modulation schemes are used to produce complicated modulated data signals. A serial to parallel transmission technique is used to transform the modulator output into a parallel data stream. On the transmitter side, the inverse FT technique is employed for getting OFDM symbols in the time domain.

In our analysis, we consider the frequency-flat fading links, and these links are *i.i.d.* Nakagami-*m* distributed with shape parameter *m* and fading link for source-to-relay, source-to-destination, and relay-to-destination fading links are given as, Ω_{SR}, Ω_{SD}, and Ω_{RD}, respectively. ISI is caused by frequency selective fading, and the CP was introduced to alleviate this problem. For improved SER performance, the CP length should be greater than the channel impulse response length. The channel impulse response of the multipath fading channel is expressed as,

$$\left\{\sum_{n=0}^{K-1} z(n)\right\}. \tag{1}$$

The received signal corresponding to the transmission of $s(n)$ is represented as [3–5],

$$y(n) = s(n) \otimes z(n) + \mathrm{N}_0(n), \tag{2}$$

where $z(n)$ is the Nakagami-*m* random variable and $\otimes$ represents the circular convolution, $\mathrm{N}_0(n)$ represents the channel noise with expected value 0 and standard deviation $\sqrt{N_0/2}$, i.e., **CN**$(0, N_0/2)$. The receiver side performs the discrete FT and CP, which have been removed,

$$Y(m) = S(m)Z(m) + \tilde{\mathrm{N}}(m) \tag{3}$$

where $Y(m), S(m), Z(m)$ and $\tilde{\mathrm{N}}(m)$ are the discrete FT of $y(n), s(n), z(n)$, and $\mathrm{N}_0(n)$, respectively. In U/L NOMA transmission, the composite signal at the BS is expressed as,

$$Y(m) = \sum_{t=1}^{M} \sqrt{P_t(n)} S_t(m) Z_t(m) + \tilde{\mathrm{N}}(m), \tag{4}$$

Where $Y(m)$ denote the received signal corresponding to the transmission of $S_t(m)$ and $\tilde{\mathrm{N}}(m)$ represents the channel noise. $P_t(n)$ represents the power allocated to the tth user on the mth subcarrier. For M subcarriers, the total power is expressed as P. The optimal power allocation factor is represented as, $\beta_t(m) = P_t(m)/P$, for tth user. The total available power is expressed as, $\sum_{t=1}^{M} \beta_t(m) = 1$. The channel is essentially a multitap channel due to multipath propagation. The channel impulse response $z_t(n)$ for tth user is expressed as, $z_t(n) = \sum_{l=1}^{K} z_{t,l}\delta(\tau - \tau_{t,l})$. Where $z_{t,l}$ represents the complex channel gain and $\tau_{t,l}$ represents the time delay of the lth multi-path. The discrete FT of the $z_t(n)$ is given as $Z_t(m)$. The total number of resolved paths are equal to 50 and fading links are *i.i.d.* Nakagami-*m* distributed.

4 DL-Based NOMA Receiver

4.1 S-LSTM RNN Architecture

In this subsection, the investigation is done for the D/L NOMA employing the DL technique over the Nakagami-*m* fading channel conditions. This DL NOMA receiver is used to detect both the user symbols in a single shot. In this work, the offline training is done for the DL NOMA receiver to get the CSI by using the simulation information symbols. The Nakagami-m fading channel coefficients are obtained with a particular fading channel profile. In the online stage, the symbol mapping is taking place, and the received data symbols have been mapped directly to their corresponding power levels. The S-LSTM technique (a type of RNN) is used in this work to enhance the detecting capacity of the NOMA receiver. Only one hidden layer and a typical feed-forward output layer make up the conventional LSTM design. The S-LSTM is an evolution of the conventional LSTM design that features many hidden LSTM layers with multiple memory cells in each layer. In an S-LSTM-based DL NOMA receiver, the subcarriers are represented as time slots in the OFDM NOMA system. Now, after considering the single time step in the S-LSTM architecture, the DL training can be done by employing multiple user detection algorithms for a particular sub-carrier.

4.2 Model Training

All seventy-two sub-carriers are included in this study, with data in the form of OFDM packets. Three OFDM symbols were considered in one OFDM packet. In the OFDM system examined, each subscriber device is assigned, two pilots. The pilot occupies the first two OFDM symbols and sends the data stream with the third OFDM symbol. The signals transmitted by multiple users are superimposed by one OFDM symbol. In simulations, both the 4-PSK and QAM complex modulated baseband data symbols are considered, and each OFDM symbol contains two bits per subcarrier. The QAM and 4-PSK symbols are generated randomly for the formation of one OFDM packet, considering the fixed number of pilot carriers. On the transmitter side, the inverse fast FT operation is performed, and a CP is added to avoid ISI. To achieve optimum SER performance, the length of the channel pulse response must exceed the length of the CP. After the CP is added to the temporal domain, the OFDM packet is transmitted via the current fade channel. The BS will receive the superimposed signal, along with the AWGN channel noise. The next stage is the training of samples, which involves creating an

FV. Since the complex modulated data symbols are considered in this work. Each symbol has real and imaginary components in the received OFDM data packet as a training sample. In this work, 90 sub-carriers are considered, and one OFDM packet consists of 4 OFDM symbols. The number of features per sample determines the dimension of the FV. The dimension of the FV for 90 sub-carriers is $90 \times 4 \times 2 = 720$. By including the relevant label in the training, the DL NOMA receiver is trained to identify the signal corresponding to the *k*th subcarrier. A label is a number that represents both users' sent symbols together. There will be 20 combinations/labels because both users are broadcasting QAM or 4-PSK signals. DNNs are created in MATLAB by connecting DL layers to the DL Toolbox. This allows users to create DL models and track their progress. The size of the input to the input layer is determined by the dimension of the real-valued FV, which is 720. There are 200 hidden units in the S-LSTM layer, which is followed by a fully linked layer with a 20-bit output size. The classification layer outputs an estimated label to map the transmitted symbols of both users at the same time, and the softmax layer applies the softmax function to the input.

5 Simulation Results

By using the simulation data, the proposed S-LSTM based NOMA detector is trained, and its performance is compared with the ML receiver and SIC receiver (both multiple user detection schemes) schemes [1–3]. Since the prior CSI improves the SER performance, the fading channel coefficients can be estimated by the MMSE and LS techniques, respectively. For various SNR regimes, the symbol error probability is measured on a per sub-carrier basis. Mitigate the effect of ISI, the channel is assumed to be quasi-static or frequency flat for both the online and online training phases. For each OFDM packet, a separate random phase shift is given to the fading channel of each UE to analyze even slight fading channel fluctuations. The target signal to interference noise ratio for both UEs is set to be 15 dB. The perfect CSI scenario is considered in the ML receiver, and this is considered a reference for examining the precision of the S-LSTM-based receiver. It has been trained using 500000 OFDM samples and 200 epochs. In the simulation, the S-LSTM-based receiver is more accurate than traditional receivers when using some training pilots, when CP is removed, or when there is non-linear clipping noise. The number of subcarriers and the duration of CP in our simulation are 90 and 25, respectively. The carrier frequency is 2.8 GHz, and the number of multiple paths is 30. The maximum delay spread is set to 25, which considers complex 4-PSK and QAM modulation symbols.

5.1 Investigation of SER for Various Values of Pilots

The PS is used in the OFDM technique for estimating the fading channel coefficients. The SER performance of the MMSE and LS receivers are depending on the number of PS used during the simulations. In simulations, the PS is known as the DL NOMA receiver, and it is used to find the channel impulse response. In this work, the impact of the number of PS is investigated for the DL NOMA receiver considering the S-LSTM algorithm. In this work, the pilot sequence consists of the 20 and 90 PS. Figure 8 depicts the SER curves for UE1 and UE2 in both scenarios, considering 4-QAM symbols. When 90 PS is utilized, both LS and MMSE approaches may produce reliable predictions, as shown in Figure 8. Nonetheless, the S-LSTM-based NOMA receiver can outperform the others. At 28 dB SNR, the decoding accuracy of the LS and MMSE algorithms significantly decreases when the number of PS is reduced to 20 for both UE1 and UE2. The DL NOMA receiver, on the other hand, can match the performance of the 90-pilot example, demonstrating that the S-LSTM-based receiver is more robust to the number of PS and can achieve better performance with fewer PS. Curves show that with a decrease

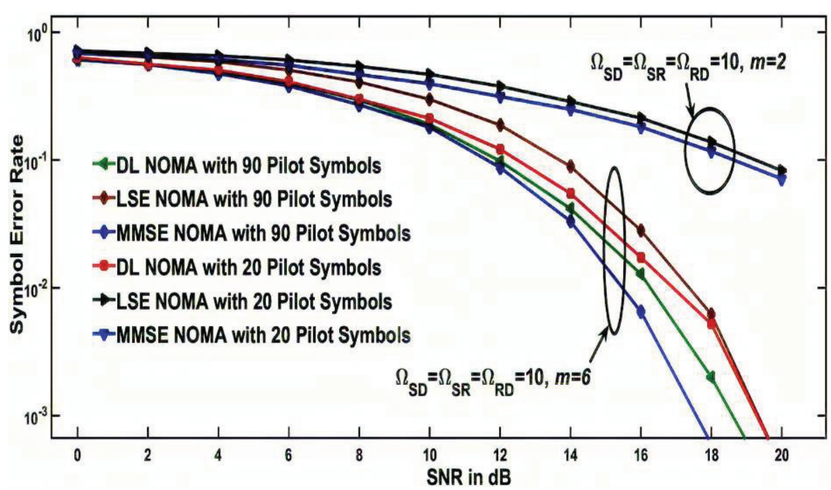

Figure 8 SER versus SNR curves of S-LSTM based DL NOMA receiver with 90 and 20 PS for various shape parameter values over the Nakagami-*m* fading channel conditions.

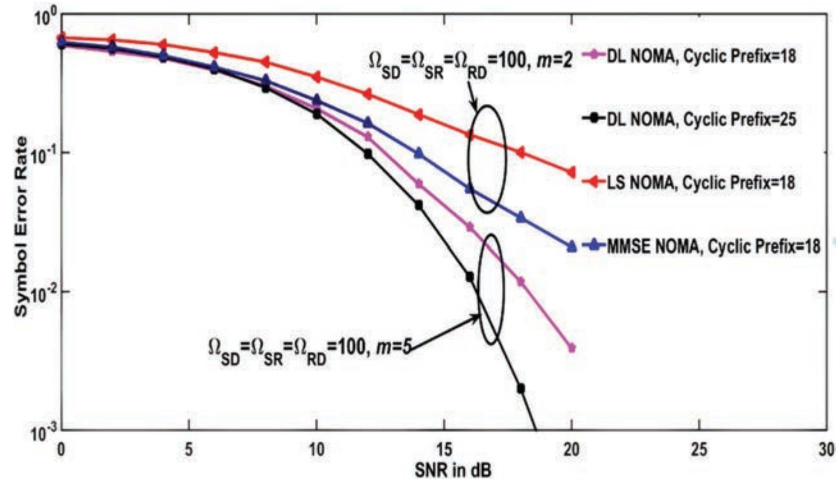

Figure 9 SER vs. SNR curves for S-LSTM based DL-NOMA receivers for various values of CP length under Nakagami-*m* fading links.

in the amount of fading (or an increase in the fading severity parameter), the SER performance improves significantly.

5.2 Investigation of SER for Various Values of CP

The CP is inserted to mitigate the effect of the ISI and to prevent non-orthogonality among the subcarriers. Figure 9 demonstrates the SER curves for UE1 and UE2 when given CPs of various lengths, considering 4-PSK complex modulated symbols. When the channel impulse response length is lower than the CP length, the DNN receiver can outperform the SIC receiver with standard LS or MMSE receivers (CP length is 25). In addition, in the case of UE2 (weak channel gain user or far user) in Figure 9, the DL NOMA receiver is robust to the signal strength of the S-LSTM-based DL NOMA receiver and propagates the estimated effect of errors in the traditional SIC scheme. In the case where the CP duration is 18, i.e., when the CP duration is less than the channel impulse duration, neither the LS nor the MMSE receiver can estimate CSI perfectly. Even with perfect channel estimation, the optimal ML-based NOMA receiver can no longer deliver the ideal answer when subjected to strong ISI effects. However, the DL NOMA receiver continues to operate effectively and can outperform the optimal ML-based NOMA receiver for both UEs. The result shows that the DL NOMA receiver is more robust to signal distortion caused by ISI and can estimate CSI perfectly from training data. The DL NOMA receiver's robustness is evaluated using channel phase fading. When the phase fading effect is ignored, the SER performance of the DL NOMA receiver is equivalent to that of the optimal ML-based NOMA receiver. In the case of a practical scenario (with phase effect), the DL receiver performs somewhat worse, demonstrating the deterioration experienced by the DL receiver when sensing phase shift packet-by-packet. In the case of strong fading channel conditions and the presence of frequency selective fading, on the other hand, the DL receiver is proven to be resistant to random phase shifts and to deliver equivalent performance to its counterpart in ideal conditions. Through simulation, it has been proven that increasing the value of the shape parameter (or decreasing the amount of fading) significantly improves the end-to-end system performance.

5.3 SER Investigation Considering the PAPR Problem

One of the issues of the OFDM system is PAPR, which is addressed by filtering and clipping. However, after using the clipping approach, we run into the problem of non-linear noise, which affects the SER performance.

$$\hat{P}(l) = \begin{cases} P(l), & \text{if } |P(l)| \leq A \\ A\exp(-j\Phi(l)) & \text{otherwise} \end{cases} \tag{5}$$

Where A and $\Phi(l)$ represent the threshold and phase shift, respectively. Figure 10 shows the error performance of the MMSE, and S-LSTM based NOMA receiver when the DNN receiver is facing non-linear noise, considering 4-QAM complex modulated symbols. When the SER performance of the DL NOMA receiver is much better than the MMSE for $SNR > 15\ dB$. It has been observed that the S-LSTM based NOMA receiver is more robust against CD. In Figure 10, it has been observed that for a large value of Ω_{RD} the system performance improves. It can be readily seen that when relay to destination channel strength is exceedingly high as compared to the source to relay and source to destination fading links, the SER performance improves because we must give more power to the SR fading link for better decoding accuracy at the relay. Apart from CP and CD, Figure 11 illustrates a comparison of MMSE, and the S-LSTM based NOMA receiver in all scenarios. The graph shows that the S-LSTM receiver performs better than the conventional NOMA receiver, but the detection performance is different under the time-invariant fading condition, as shown in the previous figures.

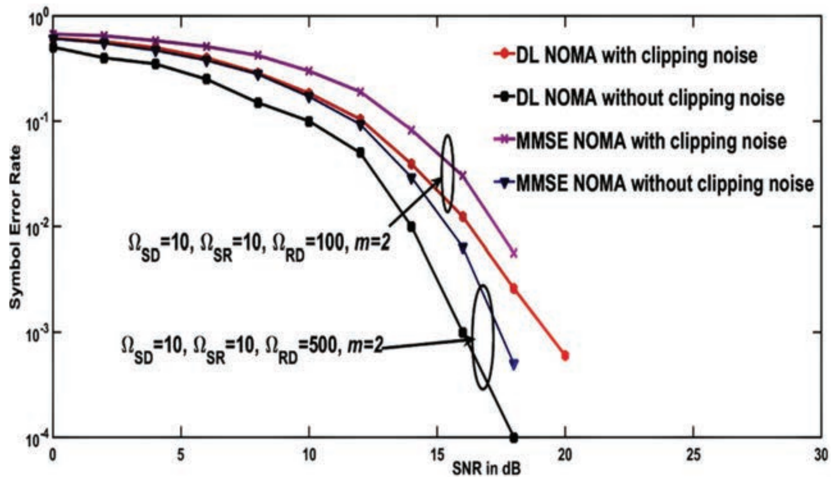

Figure 10 SER versus SNR curves of S-LSTM based NOMA receiver with and without clipping noise for various values of RD channel gain.

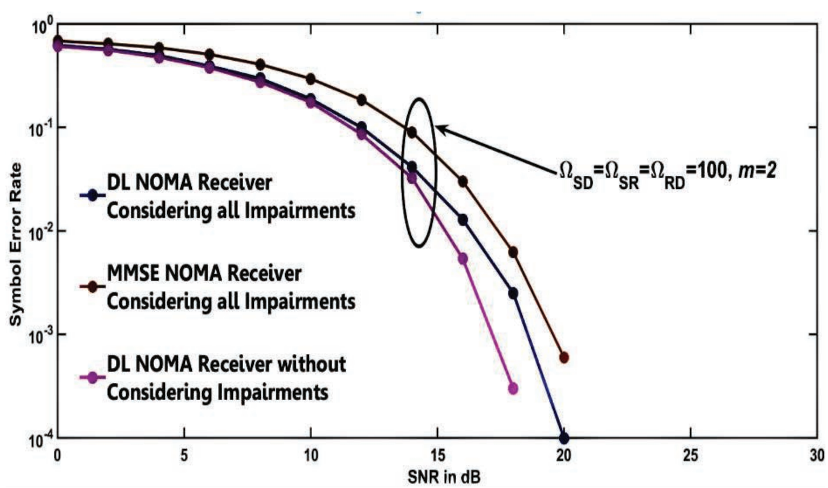

Figure 11 SER versus the SNR in dB plots considering all impairments under frequency flat Nakagami-*m* fading links.

5.4 Robustness Analysis

The CSI is estimated in the online training stage using data sets identical to those used for offline training, considering 4-PSK complex modulated symbols. In real-time propagation conditions, there is a gap between online

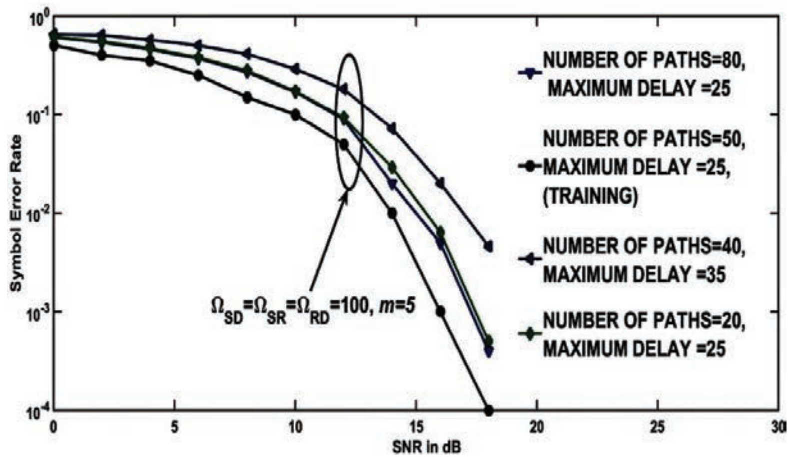

Figure 12 SER versus the SNR in dB plots considering the gaps between testing and training phases.

and offline deployments. Additionally, these differences must be sufficiently stable for the trained model. The curves in Figure 12 demonstrate the effect of change in the fading relationship statistics employed throughout the training and testing stages.

5.5 Impact of Learning Rate (LR)

The error probability performance of the S-LSTM based NOMA receiver trained with different LR's is evaluated, and the error rate curves for the two users are indicated in Figure 13. In Figure 13, lower LRs lead to lower SERs, suggesting that higher LRs will lead to faster updating of neural network weights and higher validation errors considering 4-PSK complex modulated symbols. The LR is low, but 0.003 is more accurate, for example, because it requires more updates and slows down convergence. As a trade-off between training length and training accuracy, the LR was lowered to 0.02 in all other simulated cases. Furthermore, it is demonstrated that increasing the value of the fading severity parameter enhances the SER performance considerably.

5.6 Impact of Batch Size

The training OFDM symbols are divided into packets, each of which contains fewer than the total number of training samples. Iteration is the process

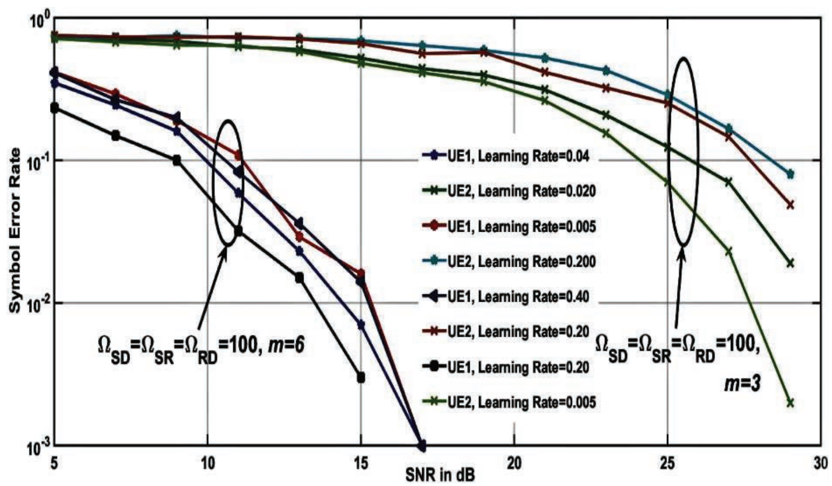

Figure 13 SER plots of DL NOMA detector for various values of the LRs over Nakagami-m fading channel.

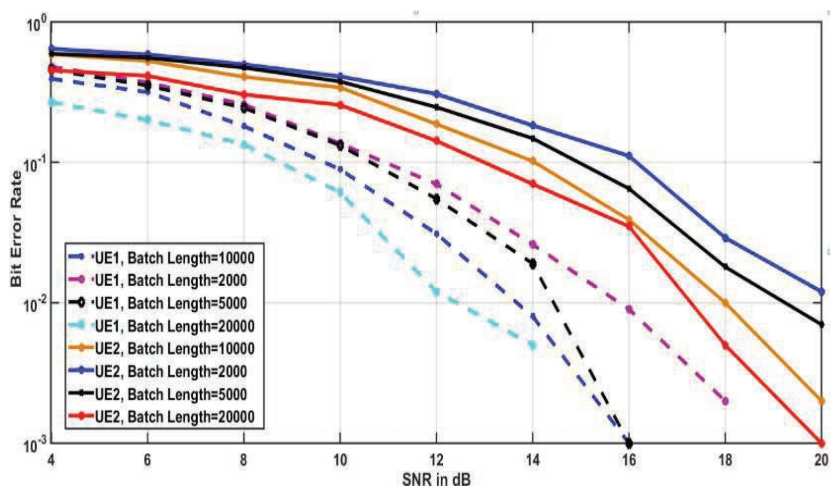

Figure 14 BER curves of DNN trained with different batch sizes over Nakagami-*m* fading channel conditions.

by which the stack propagates through the neural network in forwarding and reverse paths. It took 30 iterations to complete the epoch of the entire dataset for this study. S-LSTM processes training data in batches and uses less random-access memory (RAM) per path. Figure 14 shows the impact of different batch sizes, showing that larger batches improve DNN performance. During the training phase, small batches converge faster than large batches, so the accuracy of validation is the same. On the other hand, smaller batches result in less accurate testing. Larger batches require fewer iterations and DNN parameter changes, but more data is used to generate a more accurate gradient estimate with each update. As a result, larger batch sizes increase end-user efficiency.

6 Conclusion

A study is performed in this paper to show the DNN model's generalisation capability over the Nakagami-m fading channel circumstances for channel model parameters. With both the LS and MMSE techniques, as demonstrated in Figure 8, 90 PS provides for accurate channel estimate. Nevertheless, S-LSTM-based NOMA receivers can perform better than other NOMA receivers. With an SNR of 28 dB, reducing the number of PSs to 20 in both UE1 and UE2 will significantly reduce the decoding accuracy of the LS and MMSE algorithms. The DL NOMA receiver, on the other hand, can match the performance of the 90-pilot example. This shows that DNN is more resilient to the number of PS and can achieve better results with fewer pilots. Increasing the value of the fading severity parameter has been shown to significantly improve SER performance. Although a lower LR, e.g., 0.003, produces greater consistency, it contributes to sluggish consolidation when further improvements are required. For all the other simulation situations, the learning level has been set at 0.02, considering the trade-off between the precision of the testing and the training time.

7 Future Work

- We used different CP lengths and kinds to examine the suggested DL NOMA estimator's performance and accuracy.
- Using alternative learning algorithms, such as Adagrad, Nesterov accelerated gradient, Ada Max, and RMS prop to investigate the suggested DL NOMA estimator's performance and accuracy.
- Using robust statistics estimators such as Tukey, Log loss (cross-entropy loss), Binary Classification Loss Function, and Hinge Loss, we develop robust loss functions.

- Using crossentropyex, mean absolute error, and the sum of squares loss functions, we investigated the performance of the conventional neural network, gated recurrent units, and simple recurrent units for 84, 32, and 16 pilots.

References

[1] https://www.thalesgroup.com/en/markets/digital-identity-andsecurity/mobile/inspired/5G

[2] Kumar A, Althuwayb AA. "SIW Resonator Based Duplex Filtenna". IEEE Antennas and Wireless Propagation Letters, vol. 10, pp. 2544–2548 Oct 72021.

[3] Pandya S, Wakchaure MA, Shankar R, Annam JR. "Analysis of NOMA-OFDM 5G wireless system using deep neural network", The Journal of Defense Modeling and Simulation". March 2021. doi: 10.1177/1548512921999108.

[4] Althuwayb AA, Al-Hasan MA, Kumar A. Chaturvedi D. "Design of half-mode substrate integrated cavity inspired dual-band antenna", International Journal of RF and Microwave Computer-Aided Engineering, vol. 13, Feb. 2021. doi: 10.1002/mmce.22520.

[5] Chaudhary BP, Shankar R, Mishra RK. "A tutorial on cooperative non-orthogonal multiple access networks", The Journal of Defense Modeling and Simulation. February 2021. doi: 10.1177/1548512920986627.

[6] Chaturvedi D, Kumar A, Raghavan S. "Wideband HMSIW-based slotted antenna for wireless fidelity application", IET Microwaves, Antennas & Propagation, vol. 13, pp. 258–262, Feb 21, 2019.

[7] R. Tiwari and S. Deshmukh, "Handover Count Based MAP Estimation of Velocity with Prior Distribution Approximated via NGSIM Data-Set", IEEE Transactions on Intelligent Transportation Systems, 01 January 2021. doi: 10.1109/TITS.2020.3043888.

[8] Tiwari, Ravi, and Siddharth Deshmukh, "Analysis and design of an efficient handoff management strategy via velocity estimation in HetNets", Transactions on Emerging Telecommunications Technologies, e3642, 2019.

[9] Bhardwaj L, Mishra RK, Shankar R. "Sum rate capacity of non-orthogonal multiple access schemes with optimal power allocation", The Journal of Defense Modeling and Simulation, January 2021. doi: 10.1177/1548512920983531

[10] Shankar R. “Examination of a non-orthogonal multiple access scheme for next-generation wireless networks”, The Journal of Defense Modeling and Simulation, September 2020. doi: 10.1177/1548512920951277

[11] Vimal Bhatia, Pragya Swami, Sanjeev Sharma and Rangeet Mitra . “Non orthogonal Multiple Access: An Enabler for Massive Connectivity”, J Indian Inst Sci, vol. 100, pp. 337–348, 2020. https://doi.org/10.1007/s41745-020-00162-9

[12] Z. Elsaraf, F. A. Khan and Q. Z. Ahmed, “Deep Learning-Based Power Allocation Schemes in NOMA Systems: A Review”, 26th International Conference on Automation and Computing (ICAC), pp. 1–6, 2021. doi: 10.23919/ICAC50006.2021.9594173.

[13] Osaba, Eneko, Esther Villar-Rodriguez, Javier Del Ser, Antonio J. Nebro, Daniel Molina, Antonio LaTorre, Ponnuthurai N. Suganthan, Carlos A. Coello Coello, and Francisco Herrera. “A Tutorial On the design, experimentation and application of metaheuristic algorithms to real-World optimization problems.” Swarm and Evolutionary Computation, vol. 64, pp. 100888, 2021.

[14] Porambage, Pawani, Gürkan Gür, Diana Pamela Moya Osorio, Madhusanka Liyanage, Andrei Gurtov, and Mika Ylianttila. “The roadmap to 6G security and privacy”, IEEE Open Journal of the Communications Society, vol. 2, pp. 1094–1122, 2021.

[15] G. Gui, H. Huang, Y. Song, et al., “Deep learning for an effective non-orthogonal multiple access scheme”, IEEE Transactions on Vehicular Technology, vol. 67(9), pp. 8440–8450, 2018.

[16] A. Ahmed, Z. Elsaraf, F. A. Khan and Q. Z. Ahmed, “Cooperative Non-Orthogonal Multiple Access for Beyond 5G Networks”, IEEE Open Journal of the Communications Society, vol. 2, pp. 990–999, 2021.

[17] J. Kang, I. Kim, C. Chun, “Deep Learning-Based MIMO-NOMA With Imperfect SIC Decoding”, IEEE Systems Journal, vol. 14, pp. 3414–3417, 2020.

[18] N. E. West and T. O’Shea, ”Deep architectures for modulation recognition”, IEEE International Symposium on Dynamic Spectrum Access Networks (DySPAN), pp. 1–6, 2017. doi: 10.1109/DySPAN.2017.7920754.

[19] Peng S, Jiang H, Wang H, et al, “Modulation classification based on signal constellation diagrams and deep learning”, IEEE transactions on neural networks and learning systems, vol. 30, pp. 718–727, 2018.

[20] Y. Zeng, M. Zhang, F. Han, Y. Gong and J. Zhang, "Spectrum Analysis and Convolutional Neural Network for Automatic Modulation Recognition," in IEEE Wireless Communications Letters, vol. 8, no. 3, pp. 929–932, June 2019, doi: 10.1109/LWC.2019.2900247.

[21] H. Huang et al., "Deep Learning for Physical-Layer 5G Wireless Techniques: Opportunities, Challenges and Solutions," IEEE Wireless Communications, vol. 27, no. 1, pp. 214–222, February 2020, doi: 10.1109/MWC.2019.1900027.

[22] . M. Vaezi, G. A. Aruma Baduge, Y. Liu, A. Arafa, F. Fang and Z. Ding, "Interplay Between NOMA and Other Emerging Technologies: A Survey," in IEEE Transactions on Cognitive Communications and Networking, vol. 5, no. 4, pp. 900–919, Dec. 2019, doi: 10.1109/TCCN.2019.2933835.

[23] . M. Vaezi, R. Schober, Z. Ding and H. V. Poor, "Non-Orthogonal Multiple Access: Common Myths and Critical Questions," in IEEE Wireless Communications, vol. 26, no. 5, pp. 174–180, October 2019, doi: 10.1109/MWC.2019.1800598.

[24] . Hasan, M. K., Shahjalal, M. Islam, M. M., Alam, M. M., Ahmed, M. F. and Jang, Y. M., "The role of DL in NOMA for 5G and beyond communications", In: 2020 International Conference on Artifcial Intelligence in Information and Communication (ICAIIC), Fukuoka, Japan, pp. 303–307, 2020. https://doi.org/10.1109/ICAIIC48513.2020.9065219.

[25] . Hussain, F., Hassan, S. A., Hussain, R., & Hossain, E.,"Machine learning for resource management in cellular and IoT networks: Potentials, current solutions, and open challenges", IEEE Communications Surveys and Tutorials, vol. 22, pp. 1251–1275, 2020. https://doi.org/10.1109/COMST.2020.2964534

[26] Shankar, Ravi, T. V. Ramana, Preeti Singh, Sandeep Gupta, and Haider Mehraj. "Examination of the Non-Orthogonal Multiple Access System Using Long Short Memory Based Deep Neural Network", Journal of Mobile Multimedia, vol. 18, pp. 451–474, 2021.

[27] T. Wang, C. Wen, H. Wang, F. Gao, T. Jiang, and S. Jin, "Deep Learning for Wireless Physical Layer: Opportunities and Challenges," ArXiv preprint arXiv:1706.01151, 2017.

[28] Kumar A, Raghavan S. "Bandwidth Enhancement of Substrate Integrated Waveguide Cavity-backed Bow-tie-complementary-ring-slot Antenna using a Shorted-via", Defence Science Journal. vol. 68, issue 2, pp. 197–202, 2018.

[29] M. Kim, N. -I. Kim, W. Lee and D. H. Cho, "Deep Learning-Aided SCMA," in IEEE Communications Letters, vol. 22, no. 4, pp. 720–723, April 2018, doi: 10.1109/LCOMM.2018.2792019.
[30] H. Ye, G. Y. Li, and B. H. Juang, "Power of Deep Learning for Channel Estimation and Signal Detection in OFDM Systems," IEEE Wireless Communications Lett., vol. 7, no. 1, pp. 114–117, Feb. 2018.
[31] Z. M. Fadlullah et al., "State-of-the-Art Deep Learning: Evolving Machine Intelligence Toward Tomorrow's Intelligent Network Traffic Control Systems," IEEE Commun. Surveys & Tutorials, vol. 19, no. 4, pp. 2432–2455, May 2017.
[32] F. Tang et al., "On Removing Routing Protocol from Future Wireless Networks: A Real-time Deep Learning Approach for Intelligent Traffic Control," IEEE Wireless Commun., vol. PP, no. 99, pp. 1–7, Oct. 2017.
[33] N. Kato et al., "The Deep Learning Vision for Heterogeneous Network Traffic Control: Proposal, Challenges, and Future Perspective," IEEE Wireless Commun., vol. 24, no. 3, pp. 146–153, Jun. 2017.
[34] B. Mao et al., "Routing or Computing? The Paradigm Shift Towards Intelligent Computer Network Packet Transmission Based on Deep Learning," IEEE Trans. Comput., , vol. 66, no. 11, pp. 1946–1960, Nov. 2017.
[35] Tiwari, Ravi, and Siddharth Deshmukh. "Prior information-based Bayesian MMSE estimation of velocity in HetNets", IEEE Wireless Communications Letters, vol. 8, issue 1, pp. 81–84, 2018.
[36] Shankar R, Nandi S, Rupani A. "Channel capacity analysis of non-orthogonal multiple access and massive multiple-input multiple-output wireless communication networks considering perfect and imperfect channel state information", The Journal of Defense Modeling and Simulation. March 2021. doi: 10.1177/15485129211000139.
[37] Emir, A.; Kara, F.; Kaya, H.; Li, X. Deep learning-based flexible joint channel estimation and signal detection of multi-user OFDM-NOMA. Phys. Commun. **2021**, 48, 101443. [CrossRef].
[38] Chuan, L.; Chang, Q.; Li, X. A deep learning approach for MIMO-NOMA downlink signal detection. Sensors **2019**, 19, 2526.
[39] Yang, Y.; Gao, F.; Ma, X.; Zhang, S. Deep learning-based channel estimation for doubly selective fading channels. IEEE Access **2019**, 7, 36579–36589. [CrossRef].
[40] Mao, Z.; Shi, Y. Deep learning-based channel estimation in fog radio access networks. China Commun. **2019**, 16, 16–28. [CrossRef].

[41] Bai, Q.; Wang, J.; Zhang, Y.; Song, J. Deep Learning-Based Channel Estimation Algorithm over Time Selective Fading Channels. IEEE Trans. Cogn. Commun. Netw. **2019**, 6, 125–134. [CrossRef].
[42] Gui, G.; Huang, H.; Song, Y.; Sari, H. Deep learning for an effective nonorthogonal multiple access scheme. IEEE Trans. Veh. Technol. **2018**, 67, 8440–8450. [CrossRef].
[43] Wang, X.; Zhu, P.; Li, D.; Xu, Y.; You, X. Pilot-Assisted SIMO-NOMA Signal Detection with Learnable Successive Interference Cancellation. IEEE Commun. Lett. **2021**, 25, 2385–2389. [CrossRef].
[44] Emir, A.; Kara, F.; Kaya, H.; Yanikomeroglu, H. Deep Learning Empowered Semi-Blind Joint Detection in Cooperative NOMA. IEEE Access **2021**, 9, 61832–61852. [CrossRef].
[45] Ye, H.; Li, G.Y.; Juang, B.-H.F. Power of deep learning for channel estimation and signal detection in OFDM systems. IEEE Wirel. Commun. Lett. **2018**, 7, 114–117. [CrossRef].
[46] Aldababsa, M.; Toka, M.; Gökçeli, S.; Kurt, G.K.; Kucur, O. A Tutorial on Nonorthogonal Multiple Access for 5G and Beyond. Wirel. Commun. Mob. Comput. **2018**, 2018, 9713450. [CrossRef].

Biographies

Ravi Shankar received the bachelor's degree in Electronics and Communication Engineering from Jiwaji University Gwalior in 2006, the master's degree in wireless and communication engineering from GGSIPU, New Delhi in 2012, and the philosophy of doctorate degree in Electronics & Communication Engineering from NIT Patna in 2020, respectively. His research areas include mobile security, deep learning, and social network analysis. He has been serving as a reviewer for many highly respected journals.

Manoj Kumar Beuria working as an Assistant professor in KIIT University, Odisha, India. He received his B. Tech degree in electronics and communication engineering from National institute of technology (NIT) Rourkela. Received his MTech degree in electronics and communication from Indian Institute of Technology (IIT) Roorkee. And currently pursuing his PHD from KIIT University. He has more than seven years of teaching experience and more than two years of industry experience. He teaches Digital Signal Processing (DSP), Communication system, Information theory And Coding, Signals And Systems, and mobile communication. Now he is doing research in 5G Communication, Wireless Sensor Network, IOT And Machine Learning.

Sudhansu Sekhar Singh has received a PhD in Engineering (Wireless Communication) from Jadavpur University, Kolkata, India and a M.E. in Electronic System and Communication Engineering from R.E.C (presently NIT) Rourkela, India. He is working as a Professor in School of Electronics Engineering, KIIT University, Bhubaneswar, India. He has more than 18 years of teaching experience and 8 years of other professional experience. More than 75 (seventy-five) publications in international journals and reputed international conference proceedings are to his credit. Also, he has guided more than twenty-five PG thesis and three doctoral theses. He has also examined several doctoral dissertations. His broad research area includes but not certainly limited to wireless and mobile communication, multicarrier CDMA, MIMO-OFDM, Wireless Sensor Networks.

Farkhanda Ana received the bachelor's degree in S.S.M College of Engineering and Technology, Affiliated to Kashmir University, the master's degree in Department of Electronics and Communication, National Institute of Technology, Srinagar, and the philosophy of doctorate degree in Department of Electronics and Communication from Department of ECE, National Institute of Technology, Srinagar, respectively. She is currently working as an Assistant Professor at the Department of Electronics and Communication School of Engineering and Technology BGSB University, Rajouri, J&K-185131. Her research areas include mobile security, deep learning, and social network analysis. He has been serving as a reviewer for many highly respected journals.

Haider Mehraj received his B. Tech in Electronics and Communication Engineering from the Guru Nanak Dev University, Amritsar, India in 2009 and MTech in Communication and Information Technology from National Institute of Technology, Srinagar, India in 2011. He is currently pursuing PhD in Biometrics at the National Institute of Technology, Srinagar, India and working as Assistant Professor in BGSB University, Rajouri, India. He has several national and international publications to his credit. His research interests include Biometrics, Image Processing, Deep Learning, and Pattern Recognition.

V. Gokula Krishnan is currently working as Professor in the Department of Computer Science and Engineering in Saveetha School of Engineering, Saveetha Institute of Medical and Technical Sciences, Thandalam, Chennai, Tamil Nadu, India. He has completed his Under-Graduation (BE) in Anna University, Post-Graduation (M.Tech) in Dr. MGR University and Ph.D in Sathyabama Institute of Science and Technology, Chennai. He has more than 16 years of teaching experience in various colleges in Chennai and Hyderabad. He has published several papers in SCI/Scopus/WoS indexed journals and also he has presented various papers in National/International Conferences. His area of interest includes Computer Networks, Computer Architecture, Data Structures, Software Engineering etc. He serves as the guest editor, editorial member and also as reviewer in many reputed international journals. He is a member of Professional Bodies like ISTE, IAENG, CSI and IEEE etc.